Journal of Alabama Academy of Science, Vol.90, No. 2, November 2019

PREDICTING THE SIZE AND TIMING OF THE NEXT SOLAR CYCLE: PAPER II, BASED ON GEOMAGNETIC VALUES

Robert M. Wilson
NASA Marshall Space Flight Center, NSSTC, Huntsville, Alabama

robert.m.wilson@nasa.gov

ABSTRACT

This is the second paper in a two-part study of predicting the size and timing of the next sunspot cycle (SC)25. Paper I examined the behavior of sunspot number (*R*) as a predictor, based on specific markers as gleaned from SC24. This paper (Paper II) examines the *Aa* and *Ap* geomagnetic indices, as well as the number of disturbed days (NDD), to effect the prediction for the size and timing of SC25. Presently (as of September 2019), SC24 is in the midst of what appears to be an extended solar minimum, with *R*, *Aa*, *Ap*, and NDD all of extremely low value and the nonoccurrence of any new cycle high latitude sunspots. Paper II describes methods for estimating the size of an SC and sets upper limits to the size of SC25. A definitive prediction cannot be made at this time but can be made when the minimum values of *Aa*, *Ap*, and NDD actually become available—probably in 2020 or more likely 2021.

INTRODUCTION

In Paper I (Wilson 2019b), estimates for the length of sunspot cycle (SC)24 and the timing and size of SC25 were determined based on specific SC parameters gleaned from the behavior of the present ongoing SC24. In this paper (Paper II), the behaviors of the *Aa* and *Ap* geomagnetic indices (annual values) and the number of disturbed days (NDD)—where a disturbed day is one having an index value ≥25 nT—are examined in relation to the annual variation of sunspot number (*R*).

Geomagnetic indices, in particular, the *Aa*-index (Mayaud 1972, 1980), have been used for many years to forecast the size of the just beginning SC, typically, 2–4 years in advance of cycle maximum (e.g.,Ohl 1966, 1976; Kane 1978, 1987, 1997; Sargent 1978; Wilson 1990; Thompson 1993; Wilson and Hathaway 2006, 2008). Geomagnetic indices have generally proven to provide the most accurate prediction for the expected size of an SC in advance of its maximum occurrence.

METHODS AND MATERIALS

Annual values of *R* were taken from <http://sidc.oma.be/silo/datafiles>, and annual values of the geomagnetic indices *Aa* and *Ap* were computed from their monthly mean values taken from <http://www.geomag.bgs.ac.uk/data_service/data/magnetic_indices/aaindex.html> and <http://www.geomag.bgs.ac.uk/data_service/data/magnetic_indices/apindex.html>. The NDD for both *Aa* and *Ap* (i.e., NDD(*Aa*) and NDD(*Ap*)) were determined from the daily values given in each monthly summary. Linear regression and bivariate regression analyses, as well as Fisher's exact test for 2×2 contingency tables, were employed in this investigation.

RESULTS AND DISCUSSION

Table 1 provides a tabular summary of the solar and geomagnetic index yearly values and counts that form the basis for this study. In Table 1, the occurrences of the parametric minimum (min) and maximum (max) for each of the parameters are given in the Comments column. Table 2 gives cyclic values for each of the parameters and the parametric means and standard deviations (*sd*) for each of the parameters for SC11–SC24.

Table 1. Annual values of *R*, *Aa* and *Ap* and yearly counts of NDD(*Aa*) and NDD(*Ap*).

Year	*R*	*Aa*	*Ap*	NSD(*Aa*)	NSD(*Ap*)	Comments
SC11						
1867	13.9	–	–	–	–	R_{min}
1868	62.8	18.4	–	86	–	Aa_{min}?
1869	123.6	21.0	–	116	–	
1870	232.0	22.4	–	101	–	R_{max}
1871	185.3	21.5	–	101	–	
1872	169.2	23.8	–	125	–	Aa_{max}, NDD$(Aa)_{max}$
1873	110.1	20.3	–	107	–	
1874	74.5	14.8	–	58	–	
1875	28.3	11.4	–	32	–	
1876	18.9	9.7	–	21	–	
1877	20.7	9.1	–	19	–	
SC12						
1878	5.7	7.4	–	10	–	R_{min}
1879	10.0	7.1	–	5	–	Aa_{min}, NDD$(Aa)_{min}$
1880	53.7	11.6	–	32	–	
1881	90.5	13.7	–	52	–	
1882	99.0	23.1	–	92	–	Aa_{max}
1883	106.1	17.8	–	78	–	R_{max}
1884	105.8	14.3	–	55	–	
1885	86.3	15.6	–	55	–	
1886	42.4	20.7	–	114	–	NDD$(Aa)_{max}$
1887	21.8	16.6	–	80	–	
1888	11.2	15.6	–	75	–	
SC13						
1889	10.4	12.6	–	39	–	R_{min}
1890	11.8	10.8	–	24	–	Aa_{min}, NDD$(Aa)_{min}$
1891	59.5	17.2	–	78	–	
1892	121.7	24.3	–	115	–	Aa_{max}, NDD$(Aa)_{max}$
1893	142.0	17.1	–	81	–	R_{max}
1894	130.0	20.9	–	91	–	
1895	106.6	18.2	–	86	–	
1896	69.4	18.1	–	89	–	
1897	43.8	13.7	–	46	–	
1898	44.4	15.2	–	59	–	
1899	20.2	13.3	–	42	–	
1900	15.7	7.6	–	13	–	
SC14						
1901	4.6	6.2	–	9	–	R_{min}, Aa_{min}
1902	8.5	6.6	–	8	–	NDD$(Aa)_{min}$
1903	40.8	12.0	–	30	–	
1904	70.1	11.8	–	36	–	
1905	105.5	15.1	–	56	–	R_{max}
1906	90.1	12.6	–	42	–	
1907	102.8	16.2	–	59	–	

Year	*R*	*Aa*	*Ap*	NSD(*Aa*)	NSD(*Ap*)	Comments
1908	80.9	17.2	–	79	–	NDD(*Aa*)$_{max}$
1909	73.2	17.3	–	65	–	
1910	30.9	17.6	–	77	–	Aa_{max}
1911	9.5	16.0	–	76	–	
1912	6.0	9.0	–	17	–	
SC15						
1913	2.4	8.7	–	15	–	R_{min}, Aa_{min}, NDD(*Aa*)$_{min}$
1914	16.1	10.1	–	27	–	
1915	79.0	15.7	–	72	–	
1916	95.0	19.9	–	111	–	
1917	173.6	18.3	–	82	–	R_{max}
1918	134.6	21.7	–	127	–	NDD(*Aa*)$_{max}$
1919	105.7	22.6	–	125	–	Aa_{max}
1920	62.7	17.7	–	81	–	
1921	43.5	16.6	–	55	–	
1922	23.7	18.8	–	102	–	
SC16						
1923	9.7	10.4	–	30	–	R_{min}
1924	27.9	9.3	–	29	–	Aa_{min}, NDD(*Aa*)$_{min}$
1925	74.0	13.1	–	47	–	
1926	106.5	20.0	–	96	–	
1927	114.7	16.7	–	70	–	
1928	129.7	17.8	–	78	–	R_{max}
1929	108.2	19.5	–	99	–	
1930	59.4	28.7	–	181	–	Aa_{max}, NDD(*Aa*)$_{max}$
1931	35.1	16.9	–	85	–	
1932	18.6	19.1	11.5	111	39	
SC17						
1933	9.2	16.4	10.1	82	24	R_{min}
1934	14.6	13.5	7.2	54	9	Aa_{min}, Ap_{min}, NDD(*Aa*)$_{min}$, NDD(*Ap*)$_{min}$
1935	60.2	15.7	8.9	65	22	
1936	132.8	15.4	9.1	70	25	
1937	190.6	19.1	12.4	91	40	R_{max}
1938	182.6	23.6	15.2	116	63	
1939	148.0	23.3	16.5	115	66	
1940	113.0	23.6	16.0	118	52	
1941	79.2	25.0	16.9	123	58	
1942	50.8	21.8	13.8	127	56	
1943	27.1	25.9	16.9	161	84	Aa_{max}, Ap_{max}, NDD(*Aa*)$_{max}$, NDD(*Ap*)$_{max}$
SC18						
1944	16.1	17.9	10.8	83	36	R_{min}
1945	55.3	16.4	10.4	63	25	Aa_{min}, Ap_{min}, NDD(*Aa*)$_{min}$, NDD(*Ap*)$_{min}$
1946	154.3	25.4	18.7	113	65	
1947	214.7	25.3	18.8	129	75	R_{max}
1948	193.0	22.6	15.4	120	51	
1949	190.7	21.3	15.4	99	52	
1950	118.9	25.3	18.0	138	80	
1951	98.3	28.8	22.3	162	113	Aa_{max}, Ap_{max}
1952	45.0	28.0	21.2	168	114	NDD(*Aa*)$_{max}$, NDD(*Ap*)$_{max}$
1953	20.1	22.3	15.6	121	93	
SC19						
1954	6.6	17.3	11.0	71	26	R_{min}, Aa_{min}, Ap_{min}, NDD(*Aa*)$_{min}$
1955	54.2	17.7	11.3	83	24	NDD(*Ap*)$_{min}$
1956	200.7	24.8	18.1	144	67	
1957	269.3	29,4	20.2	157	83	R_{max}
1958	261.7	28.6	19.3	163	81	
1959	225.1	30.3	21.4	166	92	
1960	159.0	32.9	23.7	186	100	Aa_{max}, Ap_{max}, NDD(*Aa*)$_{max}$, NDD(*Ap*)$_{max}$

Year	*R*	*Aa*	*Ap*	NSD(*Aa*)	NSD(*Ap*)	Comments
1961	76.4	22.5	14.4	114	52	
1962	53.4	21.6	12.3	112	40	
1963	39.9	21.4	12.6	121	44	
SC20						
1964	15.0	17.3	10.0	81	26	R_{min}
1965	22.0	14.1	7.8	51	10	Aa_{min}, Ap_{min}, NDD(Aa)$_{min}$, NDD(Ap)$_{min}$
1966	66.8	17.4	10.3	86	21	
1967	132.9	19.9	12.0	83	34	
1968	150.0	22.6	13.5	121	41	R_{max}
1969	149.4	20.1	11.4	90	24	
1970	148.0	20.0	11.9	95	31	
1971	94.4	20.2	11.3	97	35	
1972	97.6	20.7	12.6	90	32	
1973	54.1	26.9	17.1	163	82	
1974	49.2	30.4	19.5	212	94	Aa_{max}, Ap_{max}, NDD(Aa)$_{max}$, NDD(Ap)$_{max}$
1975	22.5	23.9	14.0	140	62	
SC21						
1976	18.4	22.3	12.9	121	40	R_{min}
1977	39.3	20.3&	11.9&	97	31	NDD(Aa)$_{min}$, NDD(Ap)$_{min}$
1978	131.0	25.7	16.9	143	65	
1979	220.1	22.6	14.5	117	43	R_{max}
1980	218.9	16.7	11.1	86	27	Aa_{min}, Ap_{min}
1981	198.9	24.8	16.3	134	61	
1982	162.4	34.1	22.5	210	107	Aa_{max}, Ap_{max}, NDD(Aa)$_{max}$, NDD(Ap)$_{max}$
1983	91.0	29.7	18.6	186	89	
1984	60.5	27.0	18.8	184	84	
1985	20.6	22.7	13.7	121	42	
SC22						
1986	14.8	21.2	12.6	102	34	R_{min}
1987	33.9	19.1	10.9	83	30	Aa_{max}, Ap_{min}, NDD(Aa)$_{min}$, NDD(Ap)$_{min}$
1988	123.0	22.6	12.7	114	35	
1989	211.1	31.1	19.4	177	85	R_{max}
1990	191.8	26.6	16.3	154	65	
1991	203.3	34.3	23.4	198	108	Aa_{max}, Ap_{max}, NDD(Aa)$_{max}$, NDD(Ap)$_{max}$
1992	133.0	27.4	16.6	160	62	
1993	76.1	25.5	14.6	151	62	
1994	44.9	29.4	18.2	180	89	
1995	25.1	21.9	12.7	128	57	
SC23						
1996	11.6	18.6	9.3	78	22	R_{min}
1997	28.9	16.1	8.4	68	14	Aa_{min}, Ap_{min}, NDD(Aa)$_{min}$, NDD(Ap)$_{min}$
1998	88.3	21.2	12.0	96	33	
1999	136.3	22.3	12.5	119	48	
2000	173.9	25.4	15.1	135	53	R_{max}
2001	170.4	22.4	12.9	103	36	
2002	163.6	22.7	13.1	133	39	
2003	99.3	36.2	21.7	243	114	Aa_{max}, Ap_{max}, NDD(Aa)$_{max}$, NDD(Ap) $_{max}$
2004	65.3	23.1	13.4	128	32	
2005	45.8	23.2	13.5	123	44	
2006	24.7	16.2	8.5	73	17	
2007	12.6	15.0	7.5	71	7	
SC24						
2008	4.2	14.2	6.9	58	6	R_{min}
2009	4.8	8.7	3.9	10	0	Aa_{min}, Ap_{min}, NDD(Aa)$_{min}$, NDD(Ap)$_{min}$
2010	24.9	12.3	6.0	33	7	
2011	80.8	14.8	7.5	52	17	
2012	84.5	17.0	9.1	71	23	
2013	94.0	14.8	7.6	62	15	

Year	*R*	*Aa*	*Ap*	NSD(*Aa*)	NSD(*Ap*)	Comments
2014	113.3	15.7	7.8	61	5	R_{max}
2015	69.8	22.3	12.2	116	38	Aa_{max}, Ap_{max}, NDD(Aa)$_{max}$, NDD(Ap)$_{max}$
2016	39.8	20.0	10.5	102	26	
2017	21.7	19.4	10.3	94	29	
2018	7.0	13.9	6.9	45	7	
2019	–	–	–	(21)	(3)	
2020						

Note:

NDD means number of disturbed days, taken to be *Aa* = 25 or greater

Ap = 25 or greater

& means, the lowest value in the vicinity of R_{min}

Table 2. Solar and geomagnetic parametric values based on annual counts/averages for SC11-24.

Cycle	R_{min}	R_{max}	Aa_{min}	Aa_{max}	Ap_{min}	Ap_{max}	<*R*>	<*Aa*>	<*Ap*>	NDD (*Aa*)	NDD (*Ap*)	NDD (*Aa*) min	NDD (*Ap*) min	NDD (*Aa*) max	NDD (*Ap*) max
11	13.9	232.0	18.4?	23.8	–	–	94.5	17.2	–	849	–	–	–	125	–
12	5.7	106.1	7.1	23.1	–	–	57.5	14.9	–	648	–	5	–	114	–
13	10.4	142.0	10.8	24.3	–	–	64.6	15.8	–	763	–	24	–	115	–
14	4.6	105.5	6.2	17.6	–	–	51.9	13.1	–	554	–	8	–	79	–
15	2.4	173.6	8.7	22.6	–	–	73.6	17.0	–	797	–	15	–	127	–
16	9.7	129.7	9.3	28.7	–	–	68.4	17.2	–	826	–	29	–	181	–
17	9.2	190.6	13.5	25.9	7.2	16.9	91.6	20.3	13.0	1,122	499	54	9	161	84
18	16.1	214.7	16.4	28.8	10.4	22.3	110.6	23.3	16.7	1,196	704	63	25	168	114
19	6.6	269.3	17.3	32.9	11.0	23.7	134.6	24.7	16.4	1,317	609	71	24	186	100
20	15.0	150.0	14.1	30.4	7.8	19.5	83.5	21.1	12.6	1,309	492	51	10	212	94
21	18.4	220.1	20.3&	34.1	11.9&	22.5	116.1	24.6	15.7	1,409	589	97&	31&	210	107
22	14.8	211.1	19.1	34.3	10.9	23.4	105.7	25.9	15.7	1,447	627	83	30	198	108
23	11.6	173.9	16.1	36.2	8.4	21.7	85.1	21.9	12.3	1,370	459	68	14	243	114
24	4.2	113.3	8.7	22.3?	3.9	12.2?	49.5*	15.7*	8.1*	(726)*	(175)*	10	0	116	38
mean	10.2	173.7	13.3	25.6	8.9	20.3	84.8	19.5	13.8	1,002.8	519.4	44.5	17.9	159.6	94.9
sd	5.0	51.5	4.8	8.4	2.6	4.0	25.7	4.2	2.9	315.5	160.9	31.1	11.2	47.8	25.2

Note: * means incomplete

& means lowest value in vicinity of R_{min}

? means unsure

Figure 1 displays (a) the annual variation of *R* spanning 1867–2018, (b) the annual variation of the *Aa*-geomagnetic index spanning 1868–2018, and (c) the annual variation of the *Ap*-geomagnetic index spanning 1932–2018. In each frame, the occurrences of sunspot minimum (R_{min}) and maximum (R_{max}) are identified using unfilled and filled triangles, respectively. The numbers 11–24 identify specific SC. The circled numbers 1–5 correspond to times when changes occurred in the location of the magnetic observatories used for measuring the *Aa*-index values (see Legend).

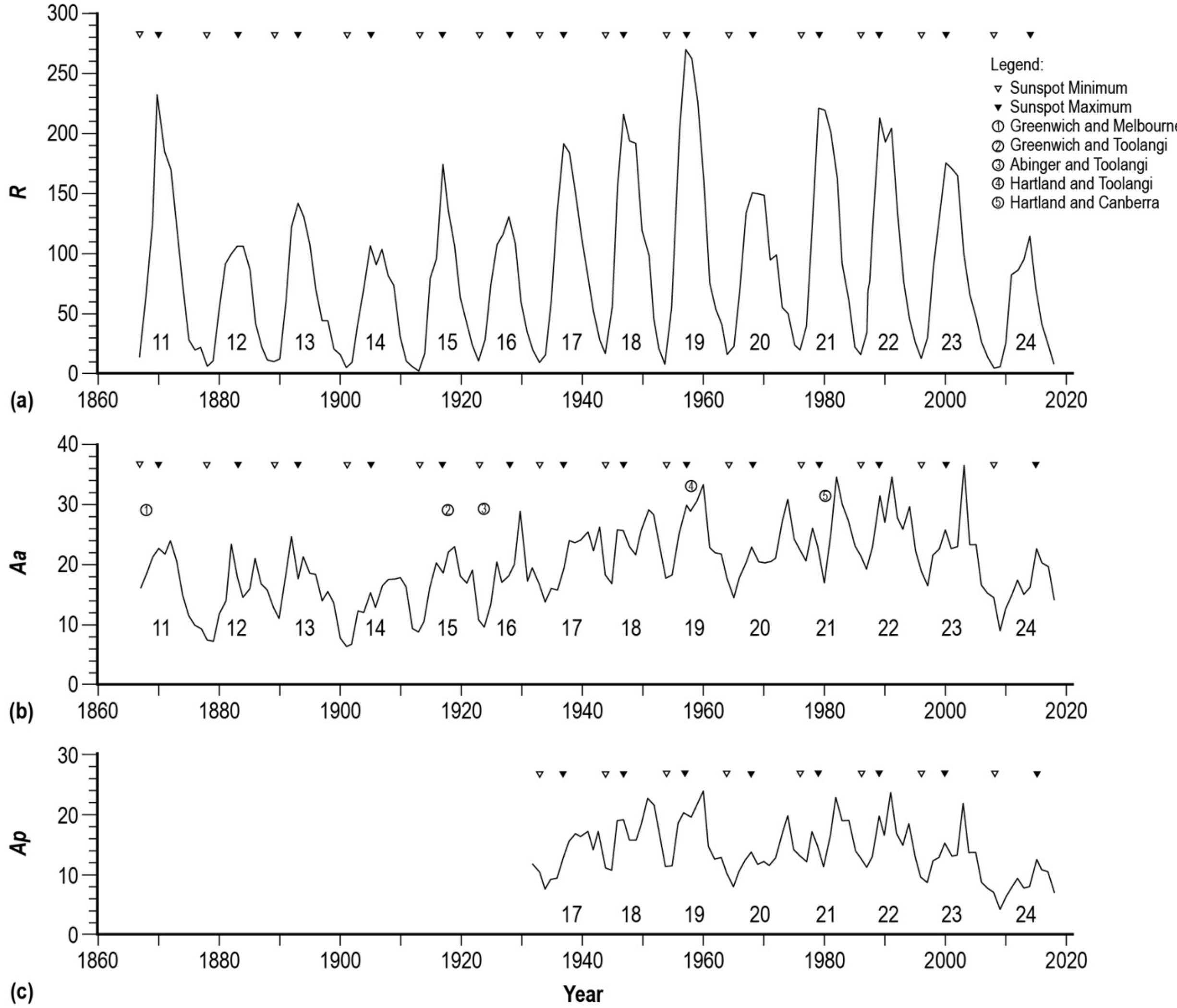

Figure 1. Annual variation of (a) *R* spanning 1867-2018, (b) *Aa* spanning 1868–2018, and (c) *Ap* spanning 1932–2018.

Recall that the *Aa*-geomagnetic index is a simple global measure of the geomagnetic fluctuations of the Earth's magnetic field due to changing conditions in the solar wind at Earth. The daily 3-hr *aa*-index (having units of nT, as does the ap index) is derived from the K indices (Patel 1977) from two nearly antipodal magnetic observatories. The resultant daily *Aa*-index is the rounded average of the eight 3-hr *aa*-index values, the monthly *Aa*-index is the rounded average of the daily *Aa*-index values, and the yearly *Aa*-index is the rounded average of the monthly *Aa*-index values. Currently (since 1980), the two observatories used in the computation of the *Aa*-index are Hartland in the United Kingdom and Canberra in Australia. Nevanlinna and Kataja (1993) have generated an extension to the *Aa*-index going back to 1844 based on magnetic observations made at the Helsinki magnetic observatory, but this extension has not been used in this analysis (except for the possible determination of $Aa_{\min}$ for SC11). The planetary *Ap*-index values are similarly calculated to that of the *Aa*-index but are based on a larger number of worldwide magnetic observatories (Rostoker 1972).

Figure 1 shows that *R* increased in strength (i.e., amplitude) from about SC12 to a peak in SC19 and then decreased in strength from SC19 through SC24. Coupled with this rise and fall in *R* has been a similar rise and fall in the geomagnetic index values, albeit with subtle differences. For example, the peak associated with geomagnetic indices is not really the occurrence of a single SC, but rather it is found to span a broader interval over several SC (i.e., SC17–SC23), with Aa_{max} for SC21–SC23 being larger than that found for SC19. Two other differences are that (1) Aa_{min} and Ap_{min} generally occur after R_{min} (i.e., usually in the year following R_{min}, true for 10 of 13 SCs, excluding SC11), and (2) Aa_{max} and Ap_{max} generally occur after R_{max} (true for 12 of 14 SCs; SC12 and SC13 had Aa_{max} the year before R_{max}). Additionally, Aa_{min} has occurred concurrently with R_{min} for only SC14, SC15, and SC19, and Aa_{min} and Aa_{max} have always occurred concurrently with Ap_{min} and Ap_{max}, respectively, for all cycles. (Based on Nevanlinna and Kataja 1993, Aa_{min} for SC11 appears to have occurred concurrently with R_{min} rather than in the year following R_{min}, having a value of about 16.0 ± 1.0 nT.)

Figure 2 displays the annual behavior of (a) NDD(*Aa*) and (b) NDD(*Ap*). The occurrences of R_{min} and R_{max} are again shown, as before, using unfilled and filled triangles, respectively. NDD$(Aa)_{min}$ generally is found to follow R_{min} by 1 year (with the exception for SC15 and SC19 and probably SC11) and NDD$(Aa)_{max}$ generally is found to follow R_{max} (the lone exception being SC13, in which it is found to precede R_{max} by 1 year). NDD$(Ap)_{min}$ is found to have occurred concurrently with NDD$(Aa)_{min}$, except for SC19 and SC24, where it is found to have followed NDD$(Aa)_{min}$ by 1 year. NDD$(Ap)_{max}$ is found to have always been concurrent with NDD$(Aa)_{max}$. As with *R* and *Aa*, NDD(*Aa*) is found to have risen from SC12 to a broad peak spanning SC17–SC23 but then to have fallen very sharply in SC24. NDD(*Aa*) was greatest (243) in 2003 (SC23), while NDD(*Ap*) was greatest (114) in 1952 (SC18) and 2003 (SC23).

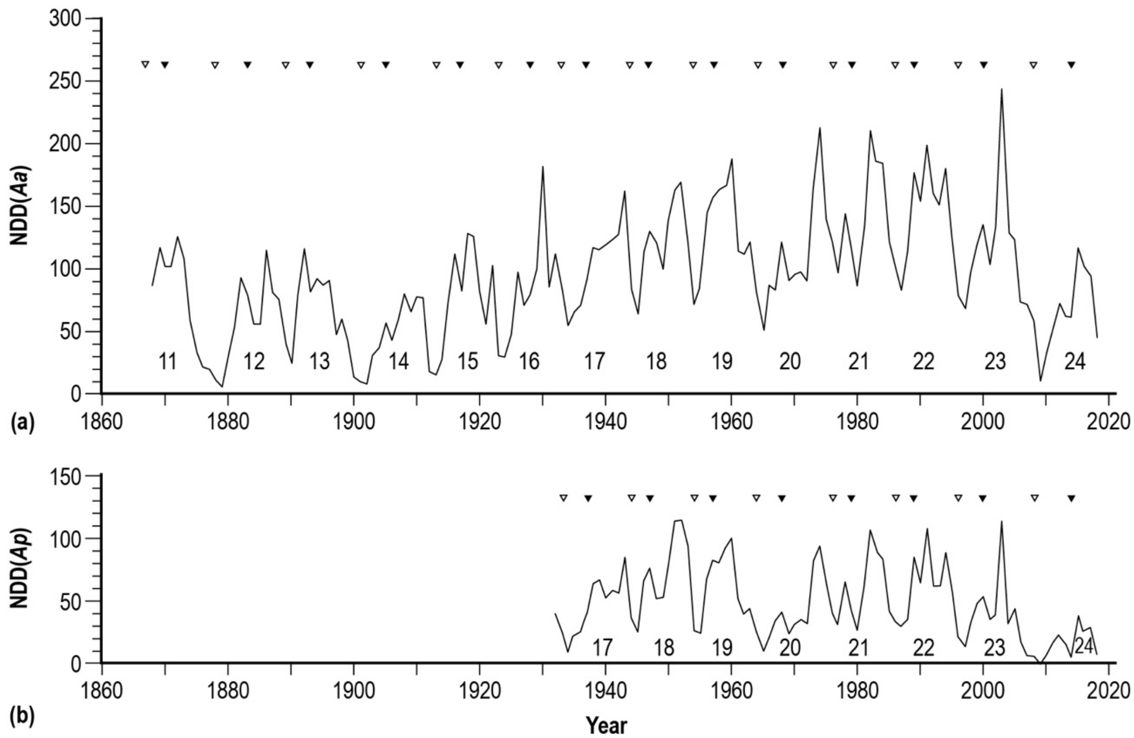

Figure 2. Annual behavior of (a) NDD(*Aa*) spanning 1868-2018 and (b) NDD(*Ap*) spanning 1932–2018.

Figure 3 depicts cyclic values of min, max, and mean for (a) R, (b) Aa, (c) Ap, and cyclic counts for (d) NDD(Aa) and NDD(Ap). For all parameters, SC24 appears to mark a return to lower values not seen since SC12–SC16. (The arrows denote that subtle changes might have to be made in the values since $Aa_{\min}$ is not exactly known for SC11 and the end of SC24 has yet to occur.)

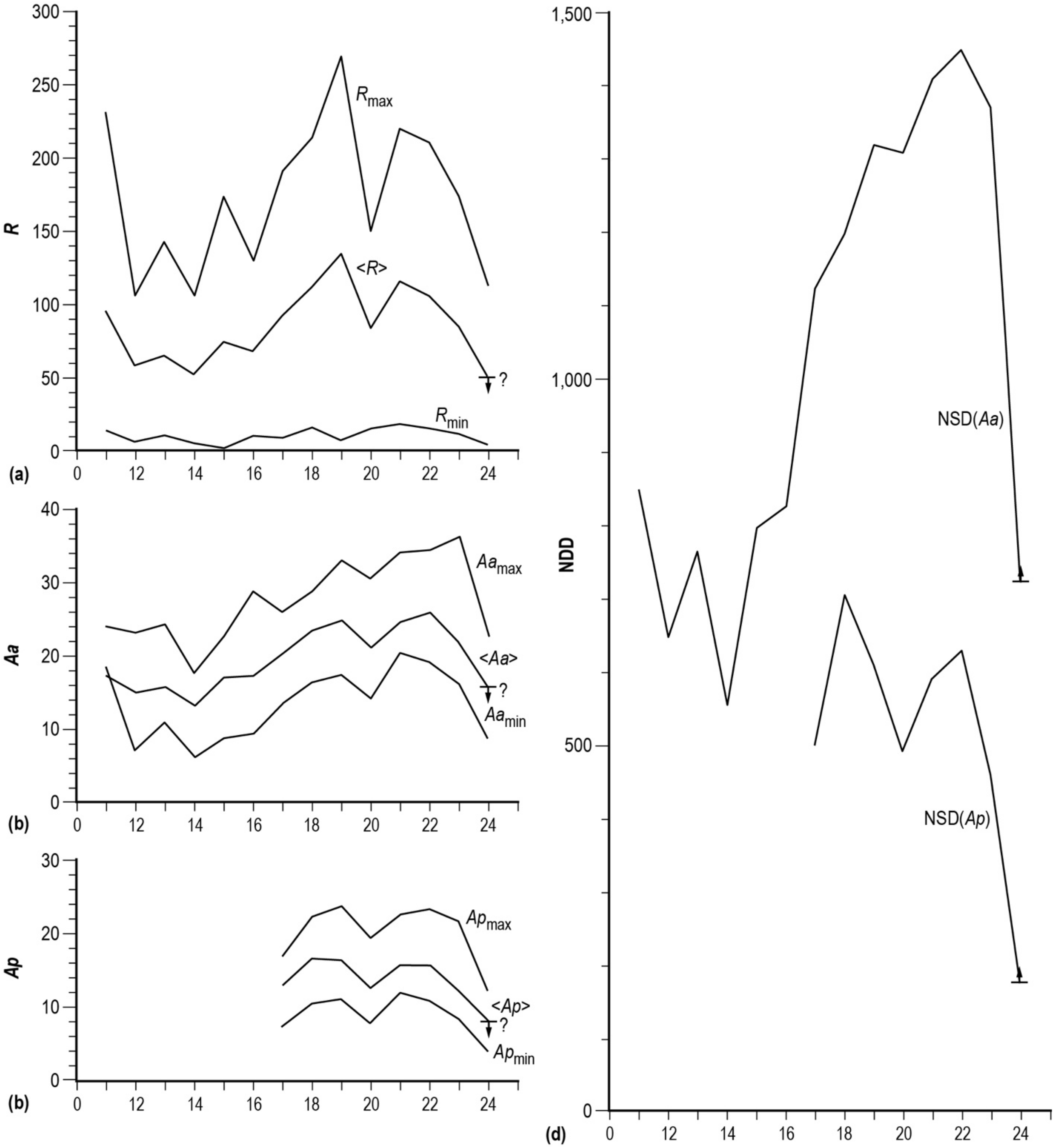

Figure 3. Cyclic values of min, max, and mean for (a) *R*, (b) *Aa*, (c) *Ap*, and cyclic counts for (d) NDD(*Aa*) and NDD(*Ap*).

Figure 4 shows the scatterplots of the maximum versus minimum values for (a) *Aa* and (b) *Ap*. Both scatterplots are inferred to be highly statistically important. Given in each frame is the inferred linear regression equation (y), the linear correlation coefficient (r), the standard error of estimate (S_{yx}), the t-statistic, and the confidence level (cl) for the inferred regression. The numbers 11–24 are the individual SCs. The result of Fisher's exact test for the 2×2 contingency tables (determined by the vertical and horizontal medians) are shown giving the probability of obtaining the observed result, or one more suggestive of a departure from independence, P. Plainly, the observed $Aa_{\min}$ and $Ap_{\min}$ provide early estimates for the later occurring $Aa_{\max}$ and $Ap_{\max}$ values. (P_o is the probability of obtaining the observed result only.)

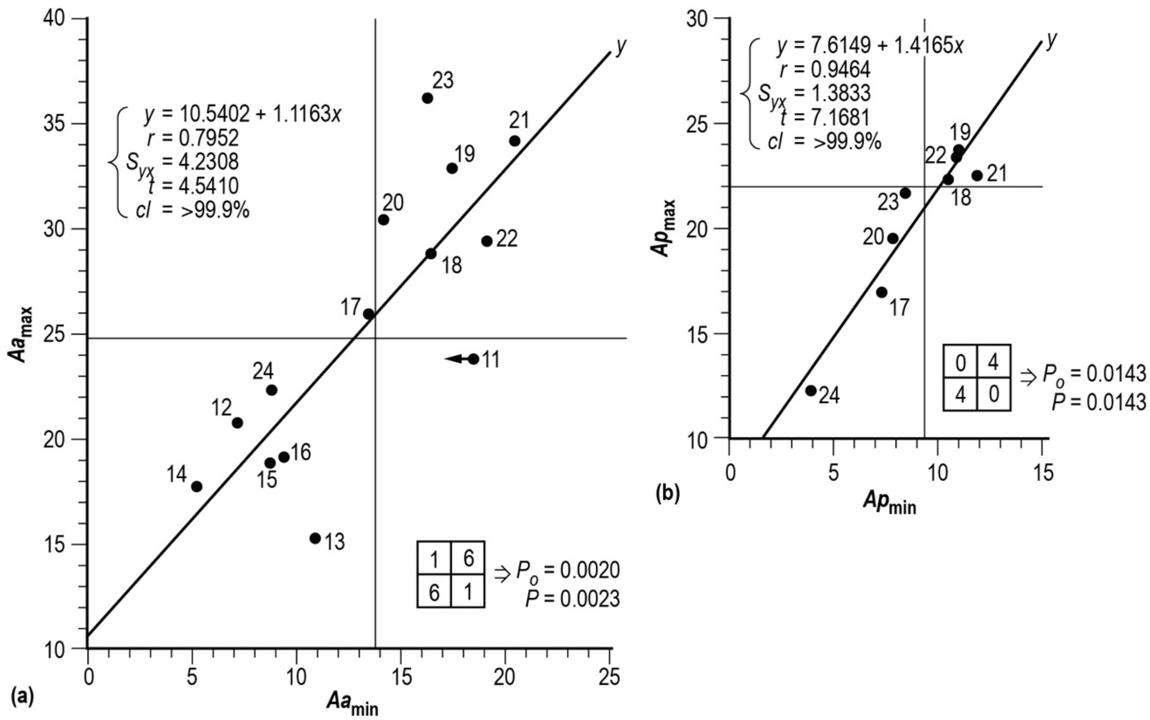

Figure 4. Scatterplots of the maximum versus minimum values for (a) *Aa* and (b) *Ap*.

Figure 5 shows scatterplots of $R_{\max}$ versus (a) $R_{\min}$, (b) $Aa_{\min}$, and (c) $Ap_{\min}$. The results of linear regression analysis and Fisher's exact test for 2×2 contingency tables are also given. Noticeable is that all three scatterplots suggest a positive correlation to exist between the minimum values and the later occurring $R_{\max}$ values. The weakest inferred correlation is the one between $R_{\max}$ and $R_{\min}$, having $r = 0.4788$, suggesting that the inferred correlation can explain only about 23% of the variance in $R_{\max}$ (i.e., $r^2 = 0.2292$). The inferred correlation has $S_{yx} = 47.0248$ and $t = 1.8892$, meaning that the inferred correlation is statistically significant at cl >90%. Based on Fisher's exact test for 2×2 contingency tables, the probability of obtaining the observed result, or one more suggestive of a departure from independence, is $P = 0.1431$, not particularly strong. As an example, assuming $R_{\min} = 2$, one estimates $R_{\max} = 133.2 \pm 47.0$ (i.e., the ±1 standard error of estimate prediction interval) using the inferred correlation and possibly $R_{\max} < 174$ based on the 2×2 contingency table (i.e., the estimated value of $R_{\max}$ would be expected to fall in the lower-left quadrant of Figure 5(a)).

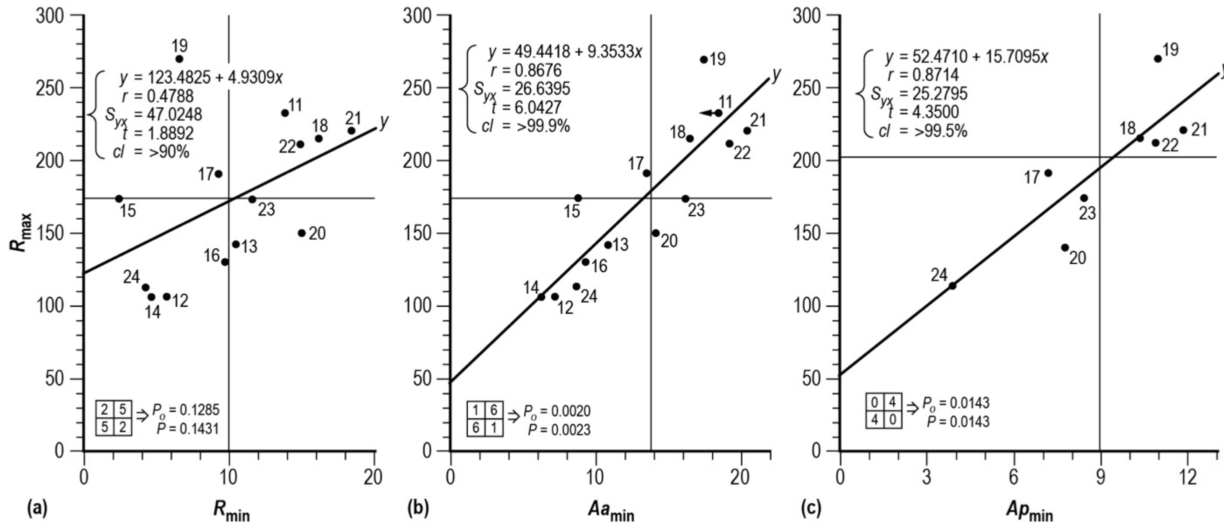

Figure 5. Scatterplots of R_{max} versus (a) R_{min}, (b) Aa_{min}, and (c) Ap_{min}.

The stronger correlations are those based on the geomagnetic indices. For R_{max} versus Aa_{min}, the inferred regression equation, $y = 49.4418 + 9.3533x$, has $r = 0.8676$, suggesting that the inferred correlation can explain about 75% of the variance in R_{max} (i.e., $r^2 = 0.7527$). The inferred correlation has $S_{yx} = 26.6395$ and $t = 6.0427$, meaning that the inferred correlation is statistically significant at cl >99.9%. Based on Fisher's exact test for 2×2 contingency tables, the probability of obtaining the observed result, or one more suggestive of a departure from independence, is $P = 0.0023$. As an example, assuming $Aa_{min} = 10$, one estimates $R_{max} = 143 \pm 26.6$ and very probably $R_{max} < 174$ (i.e., the value of R_{max} would be expected to fall within the lower-left quadrant of Figure 5(b)). For R_{max} versus Ap_{min}, one finds $r = 0.8714$, $r^2 = 0.7593$, $S_{yx} = 25.2795$, $t = 4.35$, cl >99.5%, and $P = 0.0143$. Assuming $Ap_{min} = 5$, one estimates $R_{max} = 131 \pm 25.3$ and very probably $R_{max} < 201$, again having a value of R_{max} in the lower-left quadrant of Figure 5(c).

The estimates of R_{max} are greatly improved using a bivariate fit, one combining the effects of R_{min} and either Aa_{min} or Ap_{min} (i.e., R_{max} versus y'). Figure 6 displays the scatterplots of R_{max} versus (a) R_{min} and Aa_{min} and (b) R_{min} and Ap_{min}. Both inferred correlations are highly statistically significant. As an example, assuming $R_{min} = 2$ and $Aa_{min} = 10$ nT, one computes $y' = 175.5861$ and $R_{max} = 175.6 \pm 9.2$. Assuming $R_{min} = 2$ and $Ap_{min} = 5$ nT, one computes $y' = 159.1707$ and $R_{max} = 159.2 \pm 12.1$. The overlap in the two estimates is $R_{max} = 166.4$–171.3. Such a value, if true, suggests that the hypothetical SC would be comparable in size to that of SC23 and larger than that of SC24. (The main driver in the bivariate fits is Aa_{min} and Ap_{min}; therefore, a smaller Aa_{min} or Ap_{min} yields a smaller R_{max}, while a larger Aa_{min} or Ap_{min} yield larger R_{max}.)

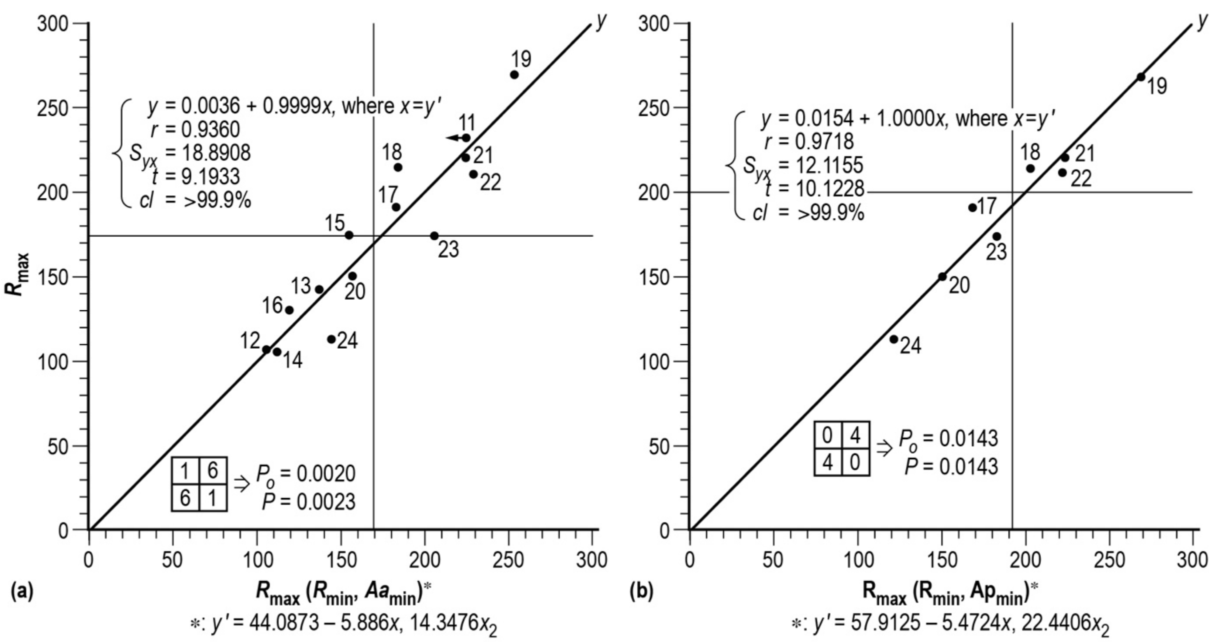

Figure 6. Scatterplots of R_{max} versus (a) R_{min} and Aa_{min}, and (b) R_{min} and Ap_{min}.

Figure 7 displays scatterplots of maximum amplitude for *R* and NDD, respectively, versus (a) and (b) NDD(Aa_{min}), and (c) and (d) NDD(Ap_{min}). All scatterplots are inferred to be statistically important, especially, those for R_{max} versus NDD(Aa_{min}) and R_{max} versus NDD(Ap_{min}).

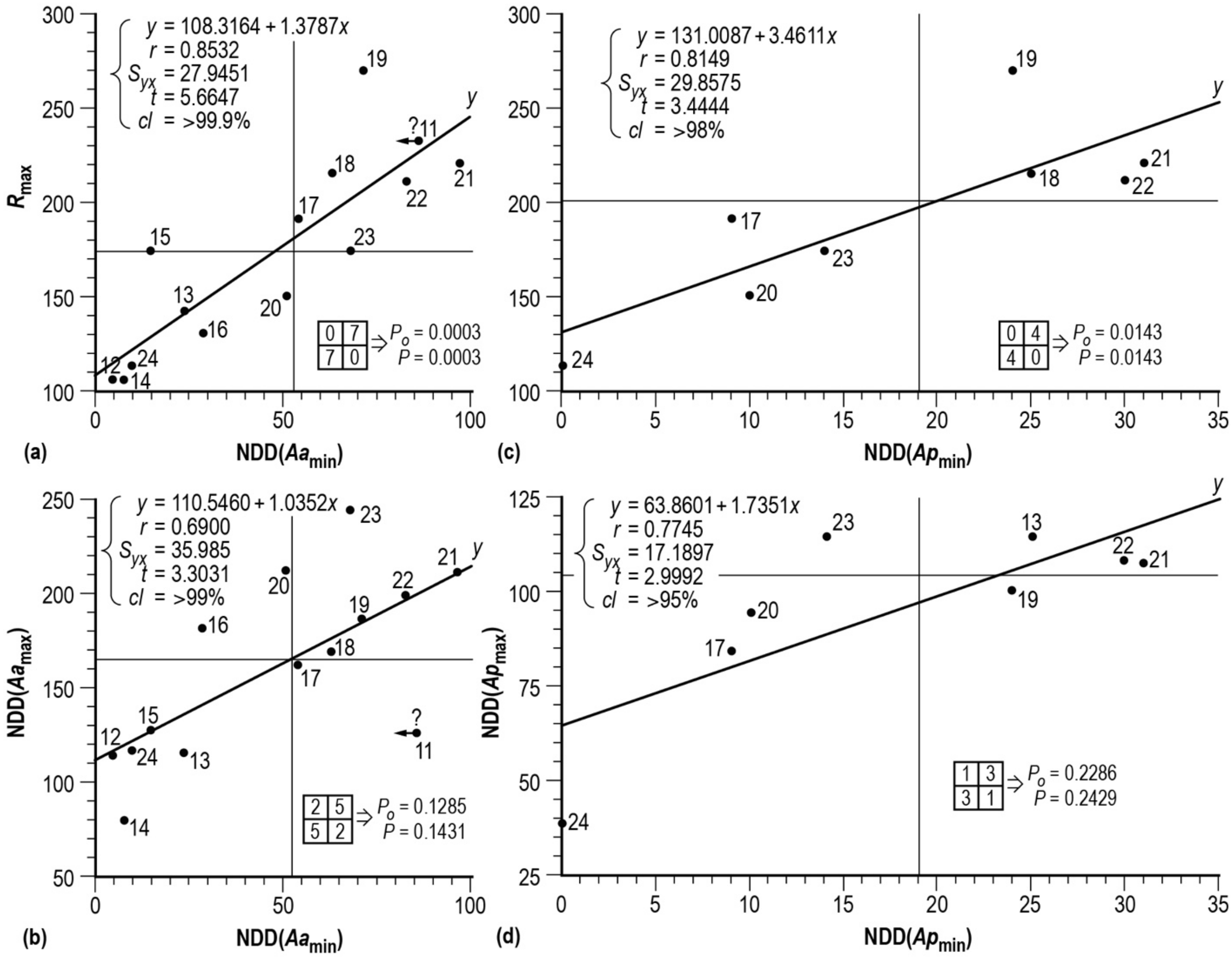

Figure 7. Scatterplots of maximum amplitude for *R* and NDD, respectively, versus (a) and (b) NDD(Aa_{min}), and (c) and (d) NDD(Ap_{min}).

Figure 8 shows the monthly variations of (a) *R*, (b) *Aa*, (c) *Ap*, (d) NDD(*Aa*), and (e) NDD(*Ap*) for the interval January 2018–August 2019 and shows previous minimum values for SC11–SC24. The trend is obviously downward for all parameters. For January–December 2018, $R = 7$, $Aa = 13.9$ nT, $Ap = 6.9$ nT, NDD(*Aa*) = 45, and NDD(*Ap*) = 7. For the interval January–August 2019, $R = 5.0$, $Aa = 10.7$ nT, $Ap = 6.1$ nT, NDD(*Aa*) = 21, and NDD(*Ap*) = 3. Therefore, one anticipates that all parameters will continue to decrease in value through 2019 into 2020, with sunspot minimum expected in 2020 or later (Wilson 2016, 2017, 2019a, b). For *R*, *Aa* and *Ap*, the observed minimum values for previous SC are identified. Values for 2019 suggest that the minimum values for SC25 will be comparable to the lowest values found for previous cycles. For NDD(*Aa*), the count for 2019 (=21, thus far) is below all previous SC, except SC12 (5), SC14 (8), SC15 (15), and SC24 (10). For NDD(Ap_{min}), the count for 2019 (3, thus far) is below all previous SC, except SC24 (0).

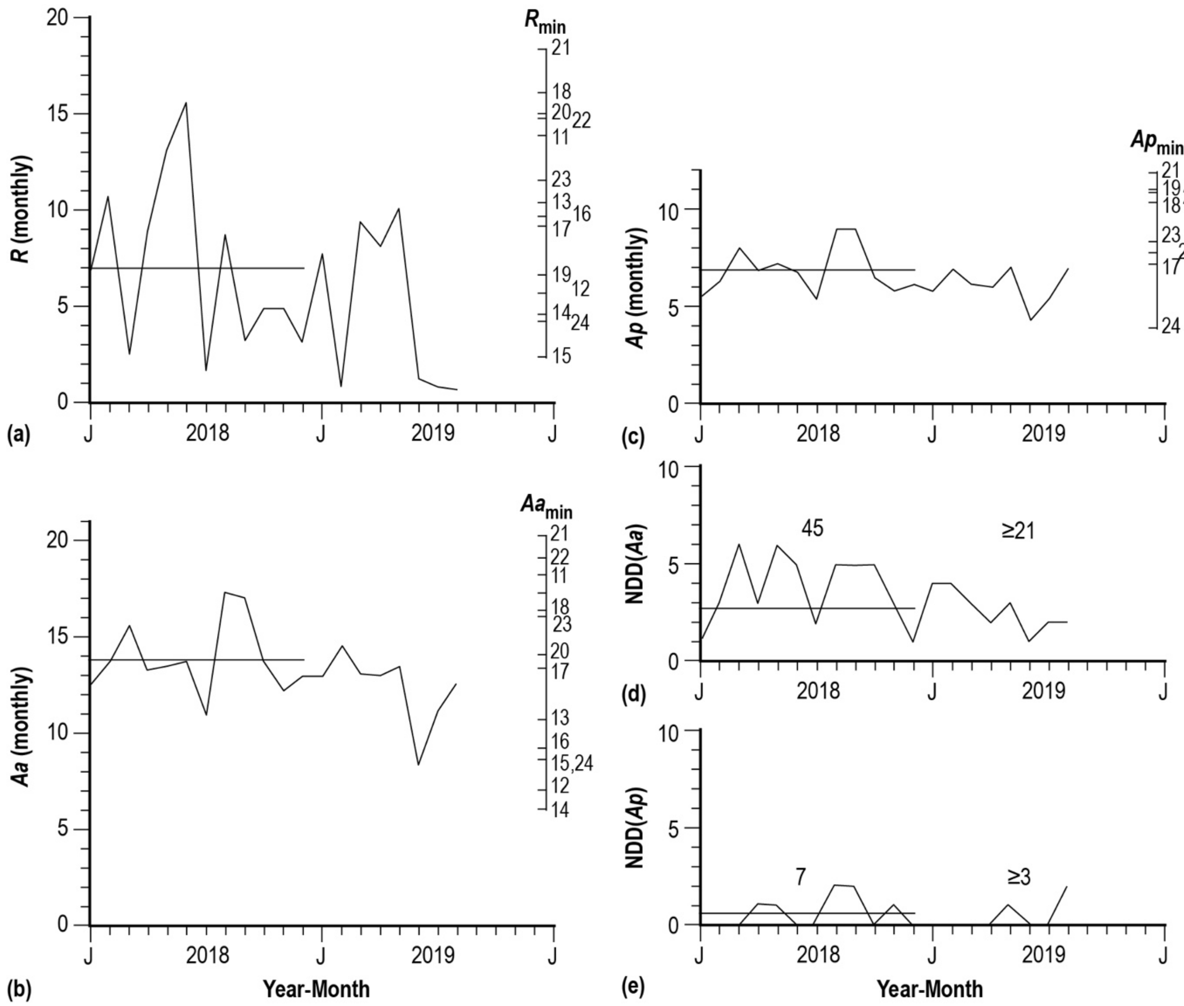

Figure 8. Monthly variations of (a) *R*, (b) *Aa*, (c) *Ap*, (d) NDD(*Aa*), and (e) NDD(*Ap*) for the interval January 2018–August 2019 and previous minimum values for SC11–SC24.

Now, Thompson (1993) noted that the NDD in the current SC (N_c, following his nomenclature) can be used to estimate R_{max} in the next SC (R_n). In particular, he compared the sum of two consecutive SC amplitudes (i.e., R_c+R_n) against N_c using the *Ap* index. In order to extend the *Ap* index backwards in time (i.e., to include SC11–SC16), the *Aa*-index was used to derive *Ap* equivalents. In the analysis here, the combined sum of two consecutive SC amplitudes (R_c+R_n) is compared separately against N_c (*Aa*) and N_c (*Ap*).

Figure 9 displays scatterplots of (R_c+R_n) versus (a) N_c (*Ap*) and (b) N_c (*Aa*). Both inferred correlations are found to be statistically significant at $cl > 95\%$. The inferred correlation between (R_c+R_n) and N_c (*Ap*) has the higher $R = 0.7890$ as compared to the correlation between ($R_c + R_n$) and N_c (*Aa*), which has $r = 0.6896$, and it also has the smaller $S_{yx} = 41.5123$. On the other hand, based on Fisher's exact test for 2×2 contingency tables, the stronger association is the one between ($R_c + R_n$) and N_c (*Aa*), having $P = 0.0251$ (due primarily to more data entries). SC24 has had far fewer N_c than any other SC on the basis of using *Ap*; however, it has slightly more N_c than

SC12 and SC14 on the basis of using *Aa*. Through August 2019, N_c (*Aa*) has totaled about 726 days, and N_c (*Ap*) has totaled about 175 days. Plainly, N_c (*Aa*) and N_c (*Ap*) for SC24 will fall within the lower-left quadrant of the scatterplots. On the basis of the inferred linear regressions, one estimates ($R_c + R_n$) >183.1 ±41.5 using N_c (*Ap*) and ($R_c + R_n$) >295.6 ±73.4 using N_c (*Aa*). Since, R_c = 113.3 for SC24, one estimates R_n >69 ±41.5 from N_c (*Ap*) and R_n >182.3 ±73.4 from N_c (*Aa*) for SC25, yielding an overlap of 108.9–111.3, inferring that SC25 might be of similar amplitude to SC24. (The overlap would be greater using larger prediction intervals. The ±1 standard error of estimate prediction interval suggests a probability of occurrence of only about 68.3%.)

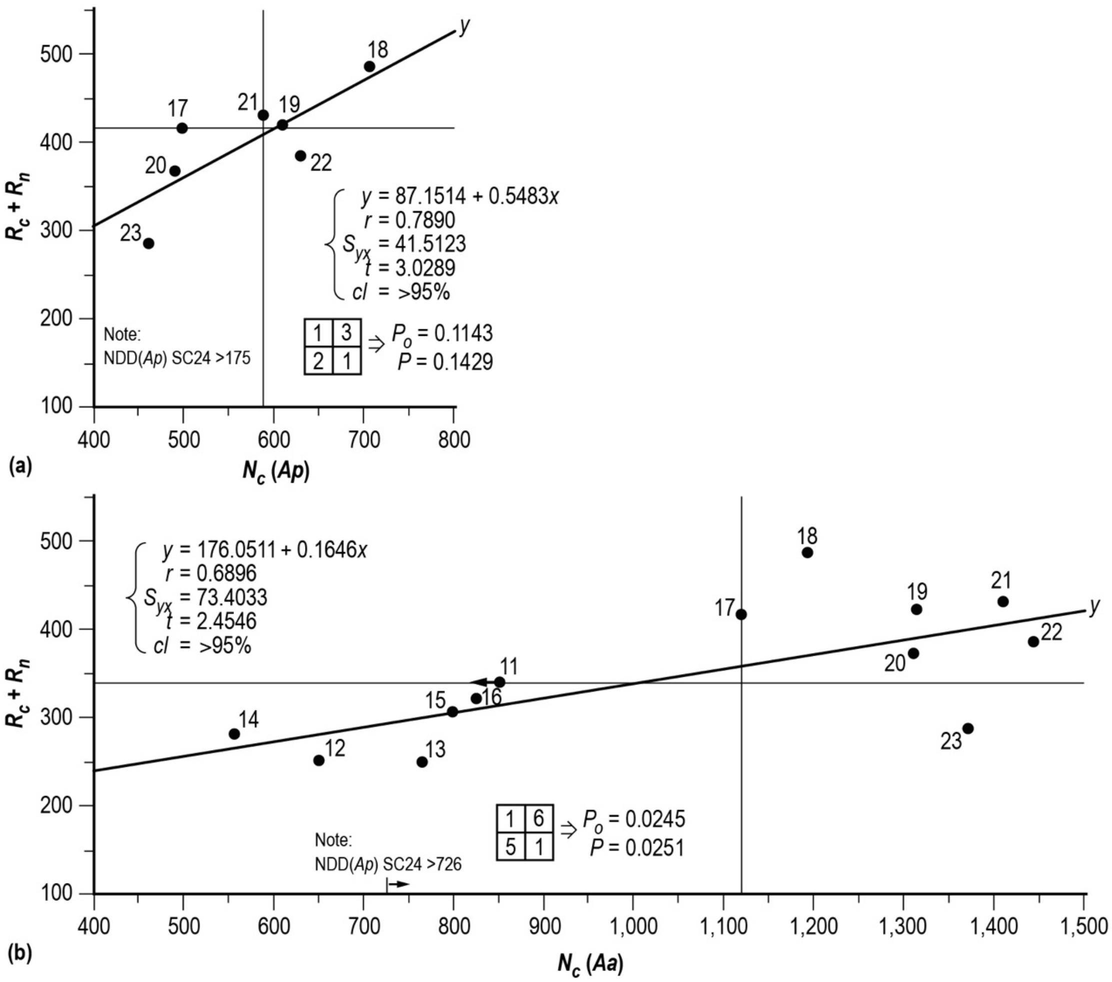

Figure 9. Scatterplots of ($R_c + R_n$) versus (a) N_c (*Ap*) and (b) N_c (*Aa*).

Previously, Wilson (2019a) showed that if the even-odd cycle amplitude effect is operative for this current even-odd cycle pair (i.e., SC24/25 is not a statistical outlier as was SC22/23), then R_{max} = 170.4 ± 13.7 for SC25 (compared to SC24 = 113.3). Similarly, based on the belief that the highest latitude spot minimum (HLSmin) occurred in 2017 and measured 19º, R_{max} = 136.2 ± 14.8 for SC25, with both predictions being ±1 standard error prediction intervals. The 90%-prediction intervals for these two estimates are 170.4 ± 24.4 and 136.2 ± 26.4, yielding an overlap of about 146.0–162.6.

In the companion paper to the present paper (Paper I, Wilson 2019b), it was noted that smoothed monthly mean sunspot number maximum *RM* averages about 224.2 ±37.2 for fast-rising SC (i.e., SC having ascent duration ASC <49 months) and only 147.3 ±43.4 for slow-rising SC (i.e., SC having ASC ≥49 months). SC24 had ASC = 64 months (and *RM* = 116.4), one month longer than SC23, inferring that SC24 is a slow-rising SC. Slow-rising SC also tend to be SC of long duration (i.e., minimum-to-minimum period PER ≥135 months), true for 9 of 12 slow-rising SC. Hence, SC24 is expected to be a long-period SC ending sometime in 2020 or later (certainly on or after March 2020 based on smoothed monthly mean sunspot number). Through September 2019, there has yet to occur any new cycle sunspots at higher latitude (i.e., ≥30º) and smoothed monthly mean sunspot number continues to decline, measuring 4.6 in March 2019. Wilson (2019b) also showed that the greatest negative change in smoothed monthly mean sunspot number (i.e., $gn\Delta R$) during the decline of SC24 measured –6.4, a value suggesting that SC24's PER = 141.1 ± 11.7 months, with 10 of 12 SC having $gn\Delta R$ = –8.7 or smaller being of long period (PER ≥135 months).

In this paper (Paper II), it has been shown that the long-term cyclic behavior of *R* is coupled with the cyclic behavior of geomagnetic indices, in particular *Aa*, *Ap*, and NDD. For all parameters, it appears that SC24 marks a return to smaller parametric values not seen since SC12–SC16, suggesting that SC25, and perhaps following SC, might well be of smaller amplitude. It has also been shown that the minimum value in the geomagnetic indices provides a reliable estimate some 2–4 years in advance for the size (R_{max}) of the ongoing SC, with minimum values in the geomagnetic indices nearly always occurring in the year following R_{min}. Linear regression correlations between R_{max} and Aa_{min} or Ap_{min} measure r = 0.87, while bivariate correlations between R_{max} and R_{min} and Aa_{min} or R_{min} and Ap_{min} measure r = 0.94 and 0.97, respectively. It is important to note that, at present, minimum amplitudes of *R*, *Aa*, *Ap*, and NDD have not yet occurred. However, based on present values of *R*, *Aa*, *Ap*, and NDD, one can estimate, as an upper limit, R_{max}. For 2019 (January–August) one computes the means for *R*, *Aa* and *Ap* to be 5.0, 12.4 nT, and 6.1 nT, respectively. Therefore, based on the inferred linear regression fits, one predicts R_{max} = 150.1 ±47.0 (based on *R*), R_{max} = 165.4 ± 26.6 (based on *Aa*), and R_{max} = 148.3 ±25.3 (based on *Ap*), all ±1 standard error of estimate prediction intervals. For the bivariate fits, one predicts R_{max} = 192.0 ±18.9 (R_{max} versus R_{min} and Aa_{min}) and R_{max} = 167.4 ±12.1 (R_{max} versus R_{min} and Ap_{min}). Actual estimates will be smaller because minimum values have not yet occurred. Figure 10 is included to show the relationship between (a) *Rm* and R_{min} and (b) *RM* and R_{max}. (*Rm* is always ≤ R_{min} and *RM* is always ≥ R_{max}.)

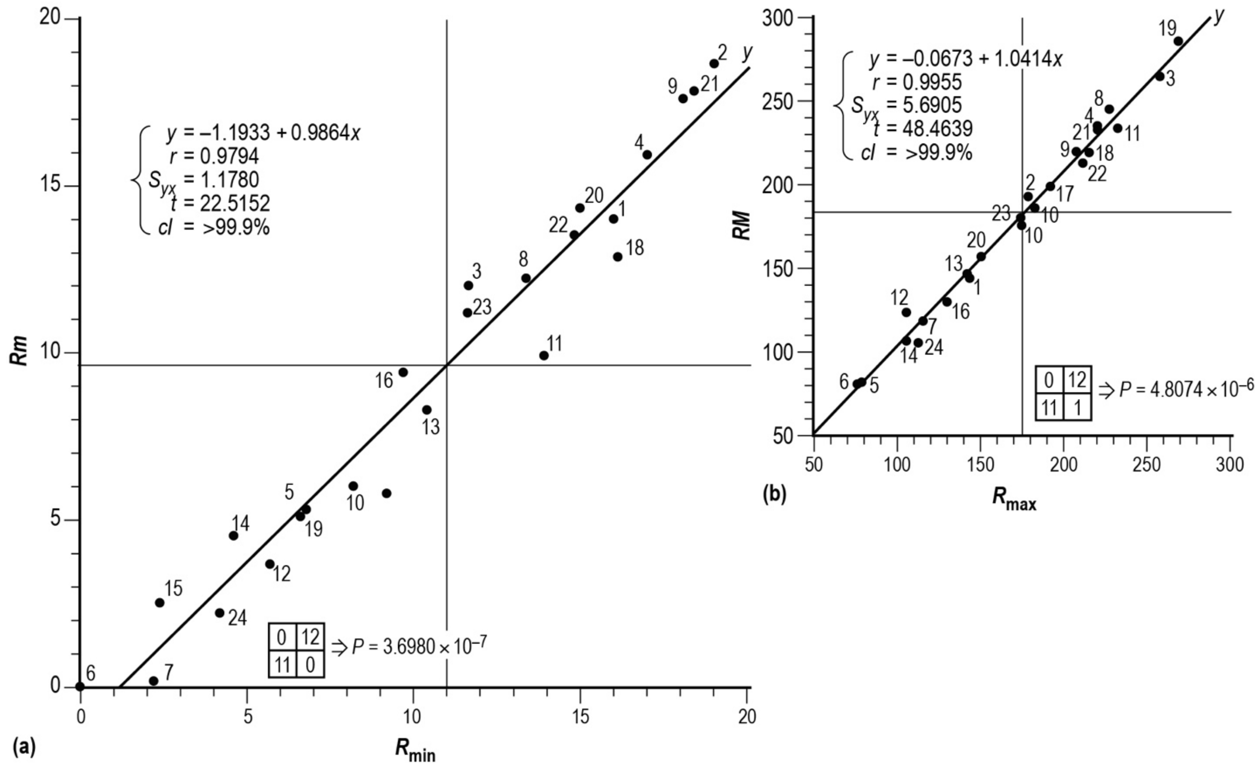

Figure 10. Scatterplots of (a) *Rm* versus R_{min} and (b) *RM* versus R_{max}.

LITERATURE CITED

Kane, R. P. 1978. Predicted Intensity of the Next Solar Maximum, *Nature*, 274, pp. 139–140.

Kane, R. P. 1987. Prediction of the Maximum Annual Mean Sunspot Number in the Coming Solar Maximum Epoch, *Solar Physics*, 108, pp. 415–416.

Kane, R. P. 1997. A Preliminary Estimate of the Size of the Coming Solar Cycle 23, based on Ohl's Precursor Method, *Geophysical Research Letters*, 24(15), pp. 1,899-1,902.

Mayaud, P. N. 1972. The aa Indices: A 100-year Series Characterizing the Magnetic Activity, *J. Geophysical Research*, 77(34), pp. 6,870-6,874.

Mayaud, P. N. 1980. Derivation, Meaning, and Use of Geomagnetic Indices, *Geophysical Monograph Series*, 22, American Geophysical Union, 154 pp.

Nevanlinna, H. and E. Kataja 1993. An Extension of the Geomagnetic Activity Index Series aa for Two Solar Cycles (1844-1868), *Geophysical Research Letters*, 20(23), pp. 2703–2706.

Ohl, A. I. 1966. Forecast of Sunspot Maximum Number of Cycle 20, *Solnice Danie*, 12, pp. 84–85.

Ohl, A. I. 1976. A Preliminary Forecast of Some Parameters of Cycle No. 21 of the Solar Activity, *Solnechnye Dannye*, 9, pp. 73–75.

Patel, V. L. 1977. 14. Solar-Terrestrial Physics, in *A. Bruzek and C. J. Durrant (eds.) Illustrated Glossary for Solar and Solar-Terrestrial Physics*, D. Reidel Publ. Co., Boston, pp. 159–193.

Rostoker, G. 1972. Geomagnetic Indices, *Reviews of Geophysics and Space Physics*, 10(4), pp. 935–950.

Sargent, H. H. 1978. A Prediction for the Next Sunspot Cycle, *28th IEEE Vehicular Technology Conference*, IEEE, Inc., New York, pp. 490–496.

Thompson, R. J. 1993. A Technique for Predicting the Amplitude of the Solar Cycle, *Solar Physics*, 148, pp. 383-388.

Wilson, R. M. 1990. On the Level of Skill in Predicting Maximum Sunspot Number: A Comparative Study of Single and Bivariate Precursor Techniques, *Solar Physic*, 125, pp. 143–155.

Wilson, R. M., 2017. Number of Spotless Days in Relation to the Timing and Size of Sunspot Cycle Minimum, *Journal of the Alabama Academy of Science*, 88(2), pp. 96-120.

Wilson, R. M. 2019a. An Examination of the Sunspot Areal Dataset, 1875-2017: Paper I, an Overview, *Journal of the Alabama Academy of Science* 90(2), pp. 31–49.

Wilson, R. M. 2019b. Predicting the Size and Timing of the Next Solar Cycle: Paper I, based on Sunspot Number, *Journal of the Alabama Academy of Science* (in press).

Wilson, R. M. and D. H. Hathaway 2006. An Examination of Selected Geomagnetic Indices in Relation to the Sunspot Cycle, NASA/TP-2006-214711, 52 pp. http://ntrs.nasa.gov/archive/nasa/casi.ntrs.nasa.gov/20070021477.pdf

Wilson, R. M. and D. H. Hathaway 2008. Using the Modified Precursor Method to Estimate the Size of Cycle 24, NASA/TP-2008-215467, 44 pp. http://ntrs.nasa.gov/archive/nasa/casi.ntrs.nasa.gov/20080043593.pdf